Title
High efficiency coronary MR angiography with nonrigid cardiac motion correction

Journal
Magnetic Resonance in Medicine, 76(5)

ISSN
0740-3194

Authors
Pang, Jianing
Chen, Yuhua
Fan, Zhaoyang
et al.

Publication Date
2016-11-01

DOI
10.1002/mrm.26332

Peer reviewed

HHS Public Access

Author manuscript

Magn Reson Med. Author manuscript; available in PMC 2017 November 01.

Published in final edited form as:

Magn Reson Med. 2016 November ; 76(5): 1345–1353. doi:10.1002/mrm.26332.

High Efficiency Coronary MRA with Non-Rigid Cardiac Motion Correction

Jianing Pang[1], **Yuhua Chen**[1,2], **Zhaoyang Fan**[1], **Christopher Nguyen**[1], **Qi Yang**[1], **Yibin Xie**[1], and **Debiao Li**[1,3]

[1]Biomedical Imaging Research Institute, Cedars-Sinai Medical Center, Los Angeles, CA, USA

[2]Computer and Information Science, University of Pennsylvania, Philadelphia, PA, USA

[3]Bioengineering, University of California, Los Angeles, CA, USA

Abstract

Purpose—To improve the coronary visualization quality of 4D coronary MRA through cardiac motion correction and iterative reconstruction.

Methods—A contrast-enhanced, spoiled gradient echo sequence with 3D radial trajectory and self-gating was used for 4D coronary MRA data acquisition at 3T. A whole-heart 16-phase cine series was reconstructed with respiratory motion correction. Non-rigid registration was performed between the identified quiescent phases and a reference. The motion information of all included phases was then used along with the corresponding k-space data to iteratively reconstruct the final image. Healthy volunteer studies (N=13) were conducted to compare the proposed method with the conventional strategy, which accepts data from a single, contiguous window out of the original 16-phase data. Apparent SNR and coronary sharpness were used as the image quality metrics.

Results—The proposed method significantly improved aSNR (11.89 ± 3.76 to 13.97 ± 5.21, P=0.005) and scan efficiency (18.8% ± 6.0% to 40.9% ± 9.7%, P<0.001), compared with the conventional strategy. Sharpness of left main (P=0.002), proximal (P=0.04) and middle (P=0.02) right coronary artery, and proximal left anterior descending (P=0.04) was also significantly improved.

Conclusion—The proposed cardiac motion-corrected reconstruction significantly improved the achievable quality of coronary visualization from 4D coronary MRA.

Introduction

Coronary arteries are challenging structures to image using MRI due to the small caliber, tortuous course, and continual motion. Therefore, successful coronary magnetic resonance angiography (MRA) requires high-resolution, whole-heart imaging, and effective motion suppression. Current free-breathing protocols use segmented acquisitions with prospective ECG and navigator gating to suppress cardiac and respiratory motion artifacts, respectively. With data accepted only from a particular cardiac (usually mid-diastole) and respiratory

Correspondence to: Debiao Li, Ph.D., Biomedical Imaging Research Institute, Cedars-Sinai Medical Center, 8700 Beverly Blvd, PACT Suite 800, Los Angeles, CA 90048, **Phone:** 310-423-7743, debiao.li@cshs.org.

(usually end-expiratory) phase, these motion suppression strategies often lead to prolonged scan time, are susceptible to variations in motion pattern, and require time-consuming setup procedures.

A number of investigators have explored the potential to relax the gating constraint and perform motion correction in order to improve the imaging efficiency while suppressing motion artifacts. Such strategy has been most prominently applied to addressing respiratory motion, in which all respiratory phases are accepted during acquisition, and the respiratory motion between respiratory phases are retrospectively corrected using information derived from self-navigation projections (1,2), image-based navigator through interleaved acquisitions (3,4), or respiratory phase resolved reconstruction from the imaging data (5,6). One (1,2) and multi-dimensional translation (3,7,8), affine (5,6), and non-rigid (9) motion models have been used to correct for respiratory motion. Compared with prospective gating, these techniques significantly reduce the scan time and largely eliminate the scan time uncertainty, as the acquisition now takes a fixed number of heartbeats to complete.

Addressing the cardiac motion using an analogous approach is more challenging. The coronary arteries move constantly. Variation in the velocity of such motion creates quiescent periods within the cardiac cycle, during which the coronary displacement is relatively small and the motion can be “frozen” given a sufficiently short acquisition window. There are typically two quiescent periods within a cardiac cycle, one during peak systole and another during mid-diastole. The duration and relative location of such periods vary considerably for different subjects, change with the heart rate, and differ between left and right coronary arteries (10–12). The conventional strategy for cardiac gating prescribes the data acceptance window such that both intra- and inter-phase motion are minimized, which means the window is usually well within one of the quiescent periods, and all other cardiac phases remain unused. Previous efforts on relaxing the inter-phase motion requirement include a 2D real-time imaging-based approach by Hardy et al with selective averaging (13), and a volume targeted approach with extended acquisition window and affine motion correction by Stehning et al (14). Due to the higher frequency (~1Hz) and highly deformable nature of cardiac motion, successful execution of the cardiac motion correction concept requires high spatiotemporal resolution, whole-heart coverage, and a realistic motion model with local deformations.

Four-dimensional (4D) whole-heart coronary MRA (15,16) is a recent development that may provide the foundation for further improving the flexibility and accuracy of cardiac motion correction. The 4D approach acquires data continuously while simultaneously records cardiac and respiratory motion information through either self-navigation alone (15) or a combination of ECG and self-navigation (16). It completely removes the scan time uncertainty, enables the flexibility to retrospectively exclude motion outliers, and offers the ability to assess the coronary arteries and left-ventricle (LV) function from a single acquisition. During image reconstruction, the respiratory motion is corrected first, and then multiple cardiac phases are reconstructed using the cardiac trigger information derived from self-navigation or ECG. Finally, an acceptance window, within which the coronary arteries remain relatively stationary, is identified and the corresponding data are used to reconstruct a high quality image for coronary visualization. The set of cardiac phases included in such

acceptance windows is always contiguous, as only one of the two typical quiescent periods, peak-systole and mid-diastole, can be included to avoid introducing artifacts from inter-phase cardiac motion. Usually 10–20% of the total data are accepted (15).

In this work, we aim to improve the cardiac gating efficiency of 4D coronary MRA by extending the cardiac acceptance window beyond a single quiescent period. First, we implemented a non-rigid registration algorithm to align all included cardiac phases to a reference phase, suppressing the inter-phase motion within the extended acceptance window. Then, we implemented an iterative reconstruction method that incorporated the motion information to yield a motion-free image using all data from the extended window. We hypothesize that the proposed method will improve the achievable quality of coronary visualization from 4D coronary MRA due to the inclusion of additional data, without introducing significant cardiac motion artifacts. We evaluated the proposed method on healthy volunteers (N=13) by comparing it with images reconstructed, without motion correction, from a conventional quiescent window, using apparent SNR and coronary sharpness as the metrics of image quality.

Methods

Data Acquisition and Cine Series Reconstruction

The general acquisition and reconstruction framework follows (15). A contrast-enhanced, spoiled gradient echo sequence with 3D radial trajectory and 1D superior-inferior (SI) self-gating (SG) was used for continuous data acquisition during free breathing. During reconstruction, the cardiac and respiratory motion signals were first extracted automatically from the multi-channel SG projection time series using principal component analysis and prior knowledge of cardiac and respiratory frequencies. Then, the k-space data were assigned to nine cardiac and six respiratory bins, taking advantage of the flexibility offered by the golden-means ordering in both azimuthal and polar angles (17). Low-resolution images were reconstructed from each bin for affine transform based, bin-by-bin respiratory motion estimation, and the motion was subsequently corrected in k-space, individually for each cardiac phase. The reference respiratory position was chosen as the one with the highest number of lines available, usually in end-expiration (18). With the respiratory motion corrected and all respiratory bins combined, the mean cardiac cycle was resampled and a 16-phase 4D image series was reconstructed. In this work, instead of the frame-by-frame non-Cartesian SENSE reconstruction used in (15), the 4D series was reconstructed using an iterative approach similar to (19) that combines sensitivity encoding and temporal regularization. The regularization parameters were empirically determined and kept constant for all subjects.

Cardiac Motion Correction

As a first step, we sought to find the cardiac phases in which both left and right coronary branches were relatively stationary. Although the quiescent phases of the major coronary arteries (LAD, LCX, and RCA) may differ, it is known that the RCA generally exhibits higher velocity and larger displacement than the left branches (11). Therefore, we identified the quiescent phases solely based on the motion of the mid-RCA segment and assumed that

the left branches would be relatively stationary if the mid-RCA were so. The reference phase for cardiac motion correction was typically chosen as the middle of the diastolic quiescent window, or middle of the systolic window if all quiescent phases are in systole. Then, a heart mask was automatically generated using a multi-atlas method and served as the region of interest (ROI) of the registration algorithm. All selected frames were also cropped to the bounding box of the heart mask in order to speed up the computation and reduce the memory requirement. A symmetric diffeomorphic algorithm (20,21) was used with cross-correlation cost function and two laplacian-filtered versions of the original image, with different variances, as additional contrasts. The estimated motion information between each moving phases and the reference, including rigid, affine, and deformable transformations, are saved for use in subsequent image reconstruction.

An example of coronary motion is presented in Fig. 1, which shows an axial slice of the 16-phase cardiac cycle reconstructed from a typical 4D acquisition. In both the systole (phases 16, 1, 2) and the diastole quiescent periods (phases 5–8), the motion of the right coronary artery (RCA) is sufficiently resolved with minimal intra-phase motion. In all other phases, the RCA moves at relatively high velocities and significant intra-phase motion can be observed. Within each quiescent period, the inter-phase cardiac motion is also relatively small, yet the shapes of the heart in systolic and diastolic phases differ significantly.

The effect of inter-phase cardiac motion correction is demonstrated in Fig. 2, which shows the same subject in Fig. 1 with all phases registered to phase 6. All cardiac phases, including the systolic ones that come with large deformations, are effectively aligned with the mid-diastolic reference frame. However, in the non-quiescent phases that carry significant intra-phase motion, including phases 3–4 and 9–15, the RCA remain blurred despite the successful registration of the larger structures. In this example, conventional gating strategy will prescribe the acceptance window to include phases 5–8. For the proposed motion correction approach, three additional phases (1, 2 and 16) may be included, leading to a 75% increase in scanning efficiency (4/16 to 7/16).

With the included phases identified and the motion information calculated, the motion-corrected reconstruction followed a previously proposed framework that iteratively inverted an encoding operator that incorporated both the sensitivity encoding operation and cardiac deformations estimated from the registration step (9,22,23):

$$\hat{\boldsymbol{x}}=\operatorname{argmin}\left\{\left|E\boldsymbol{x}-\boldsymbol{y}\right|_2^2+\lambda\left|TV\left(\boldsymbol{x}\right)\right|_1\right\} \quad [1]$$

where **x** is the unknown image in the reference cardiac phase, E is the encoding operator that maps **x** to the multi-channel, multi-cardiac phase k-space data **y**, TV() is the spatial total variation (TV) operator, and λ is the weight of the spatial TV regularization. The forward operator was implemented as follows:

$$\boldsymbol{y}_{\text{channel,phase}}=FT_{\text{phase}}\left[\boldsymbol{S}_{\text{channel}}*{T_{\text{phase}}}^{-1}\left(\boldsymbol{x}\right)\right] \quad [2]$$

where FT is the non-uniform Fourier Transform that transforms between image space and the specific non-Cartesian k-space locations of a particular cardiac phase, **S** is the self-calibrated sensitivity map, and T^{-1} is the spatial deformation from the reference to a particular cardiac phase. The backward operator, which combined all included k-space data to yield an image in the reference cardiac phase, was implemented as follows:

$$\boldsymbol{x} = \sum_{\text{channel,phase}} \boldsymbol{S}_{\text{channel}}{}^{*} * T_{\text{phase}} \left[FT^{-1} \left(\boldsymbol{y}_{\text{channel,phase}} \right) \right] \quad [3]$$

where T is the spatial transformation from a particular phase to the reference. The iterative reconstruction program was implemented using a nonlinear conjugate gradient (CG) solver. The entire image reconstruction workflow is shown in Fig. 3.

In Vivo Studies

Healthy subjects (N=13) were scanned using a clinical 3T scanner (MAGNATOM Verio, Siemens Healthcare, Erlangen, Germany) with written informed consent and IRB approval. MR data was collected using a 32-channel phased coil array (Invivo Corporation, Gainesville, FL). The pulse sequence parameters were as follows: 1-2-1 water selective RF pulse, slab-selective excitation thickness=160 mm, TR/TE=6.0/3.7 ms, flip angle = 15°, bandwidth = 449 Hz/pixel, FOV = 320^3 mm^3, matrix size = 320^3, total number of lines = 99,994, scan time = 10 minutes, contrast enhancement with a 0.20 mmol/kg Gd-BOPTA (MultiHance, Bracco Imaging SpA, Milano, Italy) injected at 0.3 mL/s before image acquisition. Image reconstruction was implemented offline using MATLAB (Mathworks, Natick, MA) with parallel computing toolbox on a workstation with 12-core Intel Xeon CPU and 96 GB memory. The image registration and motion correciton routine was implemented using the ANTS package (http://www.picsl.upenn.edu/ANTs). The images were reformatted using OsiriX (v5.8.5 32-bit, Pixmeo, Geneva, Switzerland).

Two images were reconstructed for each subject: conventional gating without cardiac motion correction (Gating), which combined data directly from a contiguous window that exhibited minimal intra- and inter-phase motion, and the proposed method, which accepted all phases with minimal intra-phase motion and combined them with inter-phase cardiac motion correction (Moco). The scan efficiency, coronary sharpness, and apparent signal-to-noise ratio (aSNR) were compared using paired Student's t-test with a significance level of 0.05. The scan efficiency was defined as the ratio between the number of cardiac phases included for reconstruction and the total number of cardiac phases. The coronary sharpness was measured at left main (LM), proximal, middle, and distal segments of left anterior descending (LAD) and right coronary arteries (RCA), and proximal left circumflex coronary artery (LCX) using the method proposed in (24), which defines sharpness as the mean of the inverse distances between the 20% and 80% point on both sides of the 1D cross-section profile of a coronary segment. The aSNR was defined as the ratio between the mean signal intensity and standard deviation of a manually drawn region of interest (ROI) in the ascending aorta, which, considering the non-linear and non-Cartesian reconstruction used here, was chosen as a surrogate of the true SNR.

Results

Fig. 4 shows the coronal maximum-intensity projection (MIP) images from three reconstructions of two example datasets: (a)(d) conventional gating without motion correction, (b)(e) all quiescent phases combined without motion correction, and (c)(f) all quiescent phases combined with motion correction. For subject 1, the quiescent phases included ones from both systole and diastole. For subject 2, all phases were from systole, with considerable inter-phase motion within the extended acceptance window. For both subjects, the proposed method improved the image quality over conventional gating through including the additional data, and suppressed motion artifacts from effective motion correction. Fig. 5 shows images from five additional subjects. The respective cardiac phases used for reconstruction are also shown. Similar improvements in coronary visualization are observed.

For the majority of the subjects in this study, the extended acceptance window included phases from both systole and diastole, and direct reconstructions from such window yielded significant artifacts similar to Fig. 4b. For this reason, we did not extend the quantitative analyses to such images and only compared Gating and Moco. The mean aSNR for Gating and Moco were 11.89 ± 3.76 and 13.97 ± 5.21, respectively. The proposed method led to a significant improvement in aSNR ($P=0.005$). Moco also led to significant improvements in sharpness of LM ($P=0.007$), proximal RCA ($P=0.04$), middle RCA ($P=0.02$), and proximal LAD ($P=0.04$), over Gating. The mean scan efficiencies for Gating and Moco were 18.8% ± 6.0% and 40.9% ± 9.7%, respectively. The proposed method led to a significant improvement in scan efficiency ($P<0.001$). All numbers are summarized in Fig. 6.

Discussion

In this work, we proposed to improve the quality of coronary visualization from 4D coronary MRA by combining data from all quiescent phases available from the 16 reconstructed phases. Potential artifacts from inter-phase cardiac motion were suppressed through non-rigid motion registration and iterative reconstruction. In vivo studies on 13 healthy volunteers showed that the proposed method significantly improved aSNR and coronary sharpness over the conventional gating strategy that only accepted data from one quiescent period.

Numerous investigations have been conducted to study the optimal placement of the cardiac acceptance window for coronary imaging. Potential quiescent periods at both systole and diastole have been identified (11,25,26). Gharib et al compared coronary MRA during systole and diastole, and suggested that a systolic window may be more suitable for tachycardic subjects (27). Uribe et al proposed to prescribe two acceptance windows in prospective ECG gating in order to reconstruct both systole and diastole from a single scan (28). Kawaji et al proposed to prescribe an extended contiguous acceptance window and retrospectively select the best subset to optimize image quality (29). Relatively few developments have been made to address inter-phase cardiac motion. Hardy et al proposed a 2D real-time imaging based technique that acquires a large number of frames and, with translation correction, selectively combines a subset where the target coronary artery appears

in the imaging plane (13). Stehning et al proposed a prospective ECG-gated, 3D volume-targeted technique that makes use of a long (240 ms) acquisition window to reconstruct four consecutive cardiac phases, which are then motion corrected with affine transform, and averaged to yield the final reconstruction (14). Our work represented major improvements over these efforts. Leveraging the whole-heart, full cardiac cycle coverage of 4D coronary MRA, the proposed method offered considerably more flexibility in selecting the cardiac phases (i.e. combining data from more than one contiguous periods), enabled accurate characterization of the highly deformable cardiac motion in 3D, and effectively corrected such motion via iterative reconstruction. Compared with the original 4D coronary MRA technique, the proposed method offered improved coronary visualization while also allowing whole-heart LV function analysis with the 4D cine series. To validate the second point, a dedicated evaluation is required regarding the accuracy of the LV function parameters obtained from the iterative 4D reconstruction.

The major factors that influence vessel sharpness include noise, undersampling artifacts, and motion. The first two may be alleviated from accepting more data into reconstruction, yet in the context of cardiac gating, this can only be done to a certain extent to avoid blurring from cardiac motion. With the proposed method, this constraint may be relaxed since now the potential blurring from inter-phase motion is suppressed by motion correction. Results from this study suggest that combining multiple, potentially non-contiguous phases with inter-phase non-rigid motion correction improves vessel sharpness over reconstructions from a smaller, contiguous set of cardiac phases. In other words, the benefit from higher SNR and lower undersampling artifacts outweighed any potential registration errors.

Due to coronary blood flow and the elasticity of the coronary wall, the size of the coronary lumen varies throughout the cardiac cycle. Previous studies using intravascular ultrasound (30,31) and MRI (32) suggested that the pulsatile variation in coronary lumen diameter is less than 5–6% for normal arteries and even less when plaque is present. Considering the size of the coronary arteries (<5 mm) and the nominal spatial resolution of the current acquisition (1.0 mm), we do not expect such variations in coronary lumen diameter to adversely affect the ability of the proposed method to perform its intended function, i.e. detecting significant coronary stenosis (>50% reduction in diameter). Further clinical validations on CAD patients are warranted.

A limitation of the current method is the need to visually select the phases in which the coronary motion is sufficiently resolved (i.e. little intra-phase motion), necessitating user interaction for the otherwise fully automated reconstruction routine. Automating this procedure is highly desirable. Several methods have been proposed in the past for automatically detecting the cardiac quiescent period from cine images, most of which are based on calculating a global inter-phase similarity metric throughout the cardiac cycle, and finding one or more acceptance windows via peak detection and thresholding (33–36). Alternatively, one may leverage the available 3D deformations calculated from the cardiac motion registration step, and use the similarity metrics between all deformed and the reference phase as the criterion for quiescent phases.

The promise of high imaging efficiency is twofold. On one hand, given a fixed imaging time, more data may be included into the reconstruction, which improves SNR and reduces undersampling artifacts. On the other hand, given a fixed k-space sampling density requirement, the minimum scan time may be shortened due to the increased efficiency. Having demonstrated the first aspect in this work, future efforts are warranted to explore the potential of scan time reduction. In our preliminary results, the mean scan efficiency is more than doubled (18.8% to 40.9%) by incorporating additional cardiac phases, which may enable significant scan time reductions. However, the potential degradation in the image quality of each cardiac phase from further undersampling may have an adverse impact on registration accuracy, and must be studied carefully.

It is also beneficial to further reduce the temporal footprint of each reconstructed cardiac phase, which is currently around 40–60 ms (for heart rates of 60–100 bpm). Assuming an intra-phase coronary displacement up to 1 mm, coronary velocities up to 17–25 mm/s may be resolved under the current temporal resolution. However, previous studies using x-ray angiography and computed tomography have reported maximum velocities of more than 100 mm/s for the RCA (10,11,37). Therefore, reconstructing a greater number of cardiac phases may allow a larger portion of the cardiac cycle to be accepted. Furthermore, a higher temporal resolution may also be helpful in the cases of arrhythmia, where the cardiac motion is more irregular.

Another potential development is to use the motion information between motion states to improve the quality of cardiac (15) or respiratory phase-resolved imaging (38). As the forward and inverse spatial transform between each moving and the reference phase are known, the transform between any two phases can be readily calculated. Therefore, it is possible to use the proposed framework to enhance the image quality of any individual phase by redefining the reference and the associated spatial transforms. An alternative approach is to reconstruct all phases jointly with temporal similarity constraint imposed on the motion corrected cardiac cycle (39,40).

Conclusion

We have developed a cardiac motion correction framework that significantly improved the imaging efficiency, aSNR, and sharpness of contrast-enhanced 4D whole-heart coronary MRA.

Acknowledgments

This project was supported in part by NIH grant numbers HL38698 and EB002623 (PI: Debiao Li, PhD) and National Science Foundation of China Grant No. 81229001 (PI: Debiao Li, PhD)

References

1. Stehning C, Bornert P, Nehrke K, Eggers H, Stuber M. Free-breathing whole-heart coronary MRA with 3D radial SSFP and self-navigated image reconstruction. Magnetic resonance in medicine. 2005; 54(2):476–480. [PubMed: 16032682]

2. Piccini D, Littmann A, Nielles-Vallespin S, Zenge MO. Respiratory self-navigation for whole-heart bright-blood coronary MRI: methods for robust isolation and automatic segmentation of the blood pool. Magnetic resonance in medicine. 2012; 68(2):571–579. [PubMed: 22213169]
3. Henningsson M, Koken P, Stehning C, Razavi R, Prieto C, Botnar RMM. Whole-heart coronary MR angiography with 2D self-navigated image reconstruction. Magnetic resonance in medicine. 2012; 67(2):437–445. [PubMed: 21656563]
4. Ingle RR, Wu HH, Addy NO, Cheng JY, Yang PC, Hu BS, Nishimura DG. Nonrigid autofocus motion correction for coronary MR angiography with a 3D cones trajectory. Magnetic resonance in medicine. 2014; 72(2):347–361. [PubMed: 24006292]
5. Bhat H, Ge L, Nielles-Vallespin S, Zuehlsdorff S, Li D. 3D radial sampling and 3D affine transform-based respiratory motion correction technique for free-breathing whole-heart coronary MRA with 100% imaging efficiency. Magnetic resonance in medicine. 2011; 65(5):1269–1277. [PubMed: 21500255]
6. Pang J, Bhat H, Sharif B, Fan Z, Thomson LE, LaBounty T, Friedman JD, Min J, Berman DS, Li D. Whole-heart coronary MRA with 100% respiratory gating efficiency: self-navigated three-dimensional retrospective image-based motion correction (TRIM). Magnetic resonance in medicine. 2014; 71(1):67–74. [PubMed: 23401157]
7. Lai P, Bi X, Jerecic R, Li D. A respiratory self-gating technique with 3D-translation compensation for free-breathing whole-heart coronary MRA. Magnetic resonance in medicine. 2009; 62(3):731–738. [PubMed: 19526514]
8. Wu HH, Gurney PT, Hu BS, Nishimura DG, McConnell MV. Free-breathing multiphase whole-heart coronary MR angiography using image-based navigators and three-dimensional cones imaging. Magnetic resonance in medicine. 2013; 69(4):1083–1093. [PubMed: 22648856]
9. Schmidt JF, Buehrer M, Boesiger P, Kozerke S. Nonrigid retrospective respiratory motion correction in whole-heart coronary MRA. Magnetic resonance in medicine. 2011; 66(6):1541–1549. [PubMed: 21604297]
10. Wang Y, Vidan E, Bergman GW. Cardiac motion of coronary arteries: variability in the rest period and implications for coronary MR angiography. Radiology. 1999; 213(3):751–758. [PubMed: 10580949]
11. Lu B, Mao SS, Zhuang N, Bakhsheshi H, Yamamoto H, Takasu J, Liu SC, Budoff MJ. Coronary artery motion during the cardiac cycle and optimal ECG triggering for coronary artery imaging. Investigative radiology. 2001; 36(5):250–256. [PubMed: 11323512]
12. Shechter G, Resar JR, McVeigh ER. Rest period duration of the coronary arteries: implications for magnetic resonance coronary angiography. Medical physics. 2005; 32(1):255–262. [PubMed: 15719976]
13. Hardy CJ, Saranathan M, Zhu Y, Darrow RD. Coronary angiography by real-time MRI with adaptive averaging. Magnetic resonance in medicine. 2000; 44(6):940–946. [PubMed: 11108632]
14. Stehning C, Bornert P, Nehrke K, Dossel O. Free breathing 3D balanced FFE coronary magnetic resonance angiography with prolonged cardiac acquisition windows and intra-RR motion correction. Magnetic resonance in medicine. 2005; 53(3):719–723. [PubMed: 15723401]
15. Pang J, Sharif B, Fan Z, Bi X, Arsanjani R, Berman DS, Li D. ECG and navigator-free four-dimensional whole-heart coronary MRA for simultaneous visualization of cardiac anatomy and function. Magnetic resonance in medicine. 2014; 72(5):1208–1217. [PubMed: 25216287]
16. Coppo S, Piccini D, Bonanno G, Chaptinel J, Vincenti G, Feliciano H, van Heeswijk RB, Schwitter J, Stuber M. Free-running 4D whole-heart self-navigated golden angle MRI: Initial results. Magnetic resonance in medicine. 2014
17. Chan RW, Ramsay EA, Cunningham CH, Plewes DB. Temporal stability of adaptive 3D radial MRI using multidimensional golden means. Magnetic resonance in medicine. 2009; 61(2):354–363. [PubMed: 19165897]
18. Piccini D, Bonanno G, Ginami G, Littmann A, Zenge MO, Stuber M. Is there an optimal respiratory reference position for self-navigated whole-heart coronary MR angiography? Journal of magnetic resonance imaging: JMRI. 2016; 43(2):426–433. [PubMed: 26174582]

19. Kim D, Dyvorne HA, Otazo R, Feng L, Sodickson DK, Lee VS. Accelerated phase-contrast cine MRI using k-t SPARSE-SENSE. Magnetic resonance in medicine. 2012; 67(4):1054–1064. [PubMed: 22083998]
20. Avants BB, Epstein CL, Grossman M, Gee JC. Symmetric diffeomorphic image registration with cross-correlation: evaluating automated labeling of elderly and neurodegenerative brain. Medical image analysis. 2008; 12(1):26–41. [PubMed: 17659998]
21. Tustison NJ, Avants BB. Explicit B-spline regularization in diffeomorphic image registration. Frontiers in neuroinformatics. 2013; 7:39. [PubMed: 24409140]
22. Batchelor PG, Atkinson D, Irarrazaval P, Hill DL, Hajnal J, Larkman D. Matrix description of general motion correction applied to multishot images. Magnetic resonance in medicine. 2005; 54(5):1273–1280. [PubMed: 16155887]
23. Usman M, Atkinson D, Odille F, Kolbitsch C, Vaillant G, Schaeffter T, Batchelor PG, Prieto C. Motion corrected compressed sensing for free-breathing dynamic cardiac MRI. Magnetic resonance in medicine. 2013; 70(2):504–516. [PubMed: 22899104]
24. Li D, Carr JC, Shea SM, Zheng J, Deshpande VS, Wielopolski PA, Finn JP. Coronary arteries: magnetization-prepared contrast-enhanced three-dimensional volume-targeted breath-hold MR angiography. Radiology. 2001; 219(1):270–277. [PubMed: 11274569]
25. Duerinckx A, Atkinson DP. Coronary MR angiography during peak-systole: work in progress. Journal of magnetic resonance imaging: JMRI. 1997; 7(6):979–986. [PubMed: 9400840]
26. Wang Y, Watts R, Mitchell I, Nguyen TD, Bezanson JW, Bergman GW, Prince MR. Coronary MR angiography: selection of acquisition window of minimal cardiac motion with electrocardiography-triggered navigator cardiac motion prescanning–initial results. Radiology. 2001; 218(2):580–585. [PubMed: 11161182]
27. Gharib AM, Herzka DA, Ustun AO, Desai MY, Locklin J, Pettigrew RI, Stuber M. Coronary MR angiography at 3T during diastole and systole. Journal of magnetic resonance imaging: JMRI. 2007; 26(4):921–926. [PubMed: 17896391]
28. Uribe S, Hussain T, Valverde I, Tejos C, Irarrazaval P, Fava M, Beerbaum P, Botnar RM, Razavi R, Schaeffter T, Greil GF. Congenital heart disease in children: coronary MR angiography during systole and diastole with dual cardiac phase whole-heart imaging. Radiology. 2011; 260(1):232–240. [PubMed: 21493790]
29. Kawaji K, Foppa M, Roujol S, Akcakaya M, Nezafat R. Whole heart coronary imaging with flexible acquisition window and trigger delay. PloS one. 2015; 10(2):e0112020. [PubMed: 25719750]
30. Ge J, Erbel R, Gerber T, Gorge G, Koch L, Haude M, Meyer J. Intravascular ultrasound imaging of angiographically normal coronary arteries: a prospective study in vivo. British heart journal. 1994; 71(6):572–578. [PubMed: 8043342]
31. Weissman NJ, Palacios IF, Weyman AE. Dynamic expansion of the coronary arteries: implications for intravascular ultrasound measurements. American heart journal. 1995; 130(1):46–51. [PubMed: 7611122]
32. Kelle S, Hays AG, Hirsch GA, Gerstenblith G, Miller JM, Steinberg AM, Schar M, Texter JH, Wellnhofer E, Weiss RG, Stuber M. Coronary artery distensibility assessed by 3.0 Tesla coronary magnetic resonance imaging in subjects with and without coronary artery disease. The American journal of cardiology. 2011; 108(4):491–497. [PubMed: 21624552]
33. Jahnke C, Paetsch I, Nehrke K, Schnackenburg B, Bornstedt A, Gebker R, Fleck E, Nagel E. A new approach for rapid assessment of the cardiac rest period for coronary MRA. Journal of cardiovascular magnetic resonance: official journal of the Society for Cardiovascular Magnetic Resonance. 2005; 7(2):395–399. [PubMed: 15881520]
34. Rasche V, Hombach V, Kunze M, Manzke R, Merkle N, Spiess J. Automatic extraction of the low-motion phases of the heart. 2007:2545.
35. Ustun A, Desai M, Abd-Elmoniem KZ, Schar M, Stuber M. Automated identification of minimal myocardial motion for improved image quality on MR angiography at 3 T. AJR American journal of roentgenology. 2007; 188(3):W283–290. [PubMed: 17312038]
36. Huang TY, Tseng YS, Chuang TC. Automatic calibration of trigger delay time for cardiac MRI. NMR in biomedicine. 2014; 27(4):417–424. [PubMed: 24478224]

37. Achenbach S, Ropers D, Holle J, Muschiol G, Daniel WG, Moshage W. In-plane coronary arterial motion velocity: measurement with electron-beam CT. Radiology. 2000; 216(2):457–463. [PubMed: 10924570]

38. Deng Z, Pang J, Yang W, Yue Y, Sharif B, Tuli R, Li D, Fraass B, Fan Z. Four-dimensional MRI using three-dimensional radial sampling with respiratory self-gating to characterize temporal phase-resolved respiratory motion in the abdomen. Magnetic resonance in medicine. 2015; doi: 10.1002/mrm/25753

39. Lingala SG, DiBella E, Jacob M. Deformation corrected compressed sensing (DC-CS): a novel framework for accelerated dynamic MRI. IEEE Trans Med Imaging. 2015; 34(1):72–85. [PubMed: 25095251]

40. Royuela-Del-Val J, Cordero-Grande L, Simmross-Wattenberg F, Martin-Fernandez M, Alberola-Lopez C. Nonrigid groupwise registration for motion estimation and compensation in compressed sensing reconstruction of breath-hold cardiac cine MRI. Magnetic resonance in medicine. 2015; doi: 10.1002/mrm.25733

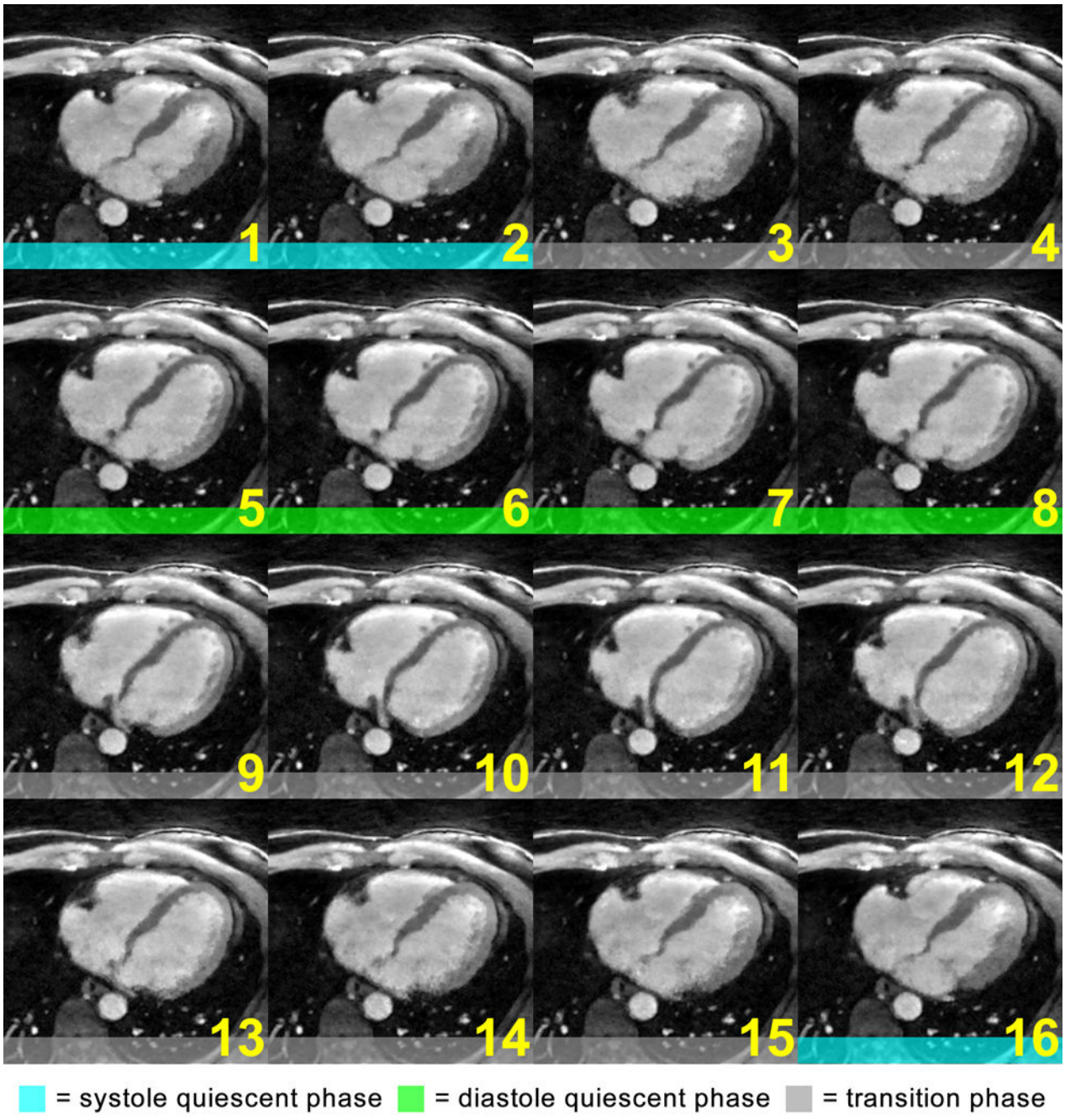

Fig. 1.

Motion of a mid-RCA segment throughout the entire cardiac cycle reconstructed from a 4D coronary MRA acquisition: the coronary artery stayed relatively still during phases 1, 2, and 16, the systolic quiescent period, and phases 5–8, the diastolic quiescent period. All other phases exhibit significant intra-phase motion as evidenced by the blurry RCA segment. The conventional gating strategy places the acceptance window within one of the quiescent periods, e.g. phases 5–8 for this subject, while discarding the data from the other phases.

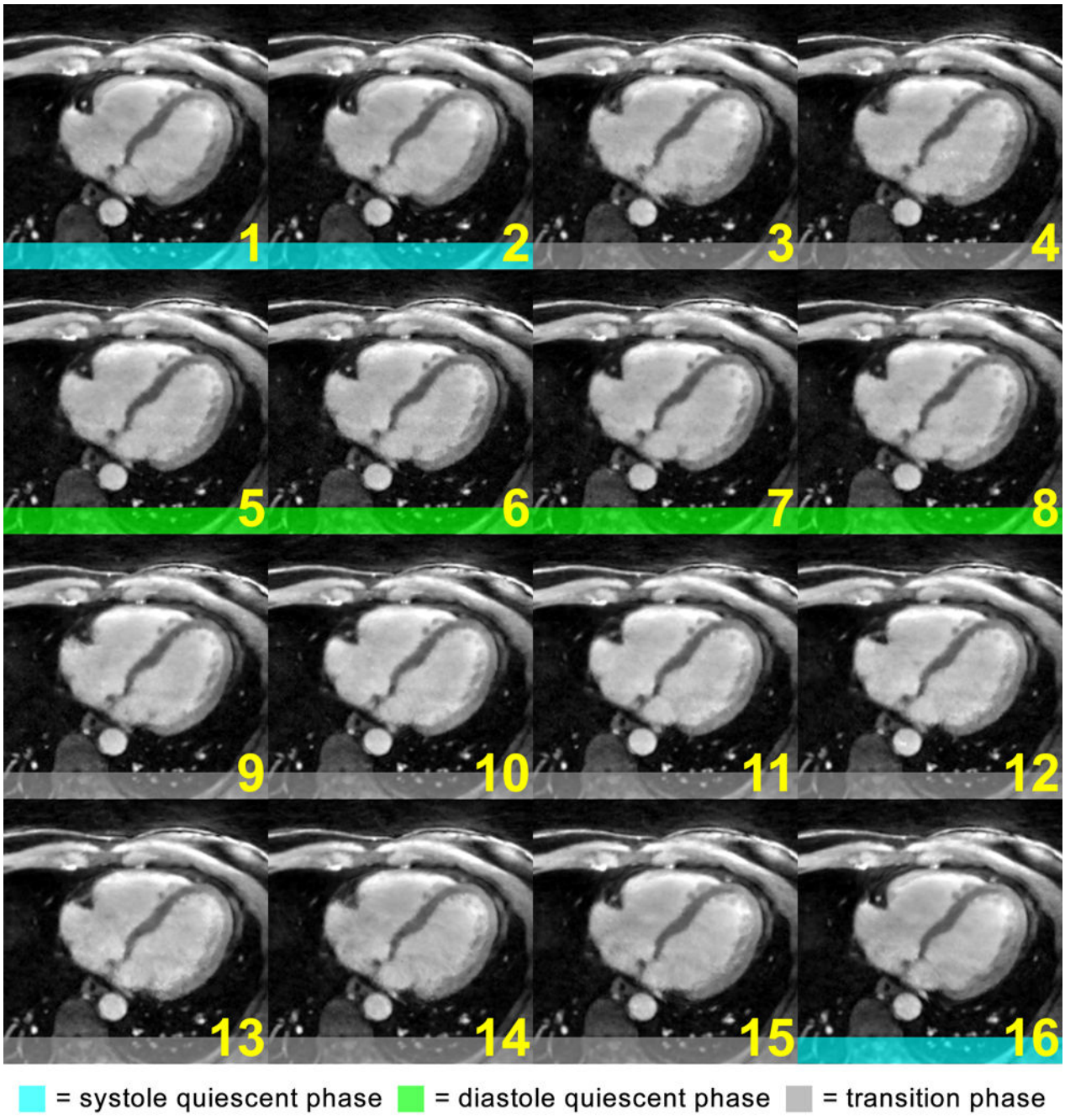

Fig. 2.

The cardiac cycle from the same subject in Fig. 1, after non-rigid motion correction: all phases were registered with the reference, phase 6, and may be combined without significant artifacts from inter-phase cardiac motion. However, the intra-phase motion in phases 3, 4, 9–15, could not be corrected. Therefore, these phases would not be included in the subsequent reconstruction.

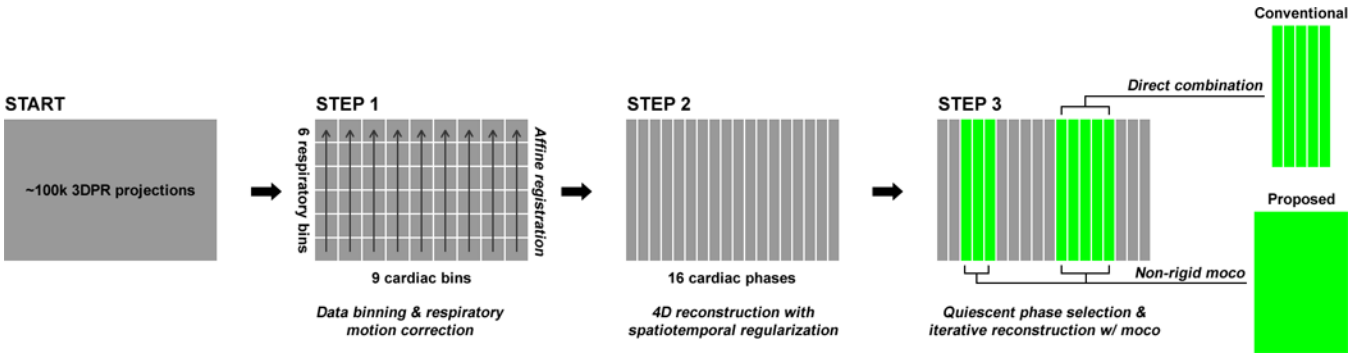

Fig. 3.

The proposed reconstruction workflow: starting with the continuously acquired 3DPR k-space data, first the dataset is segmented into multiple cardiac/respiratory phases, and the respiratory motion is corrected using affine transform separately for each cardiac phase. Then, a 16-phase cardiac cycle is reconstructed. Last, the quiescent phases are identified and combined with or without motion correction.

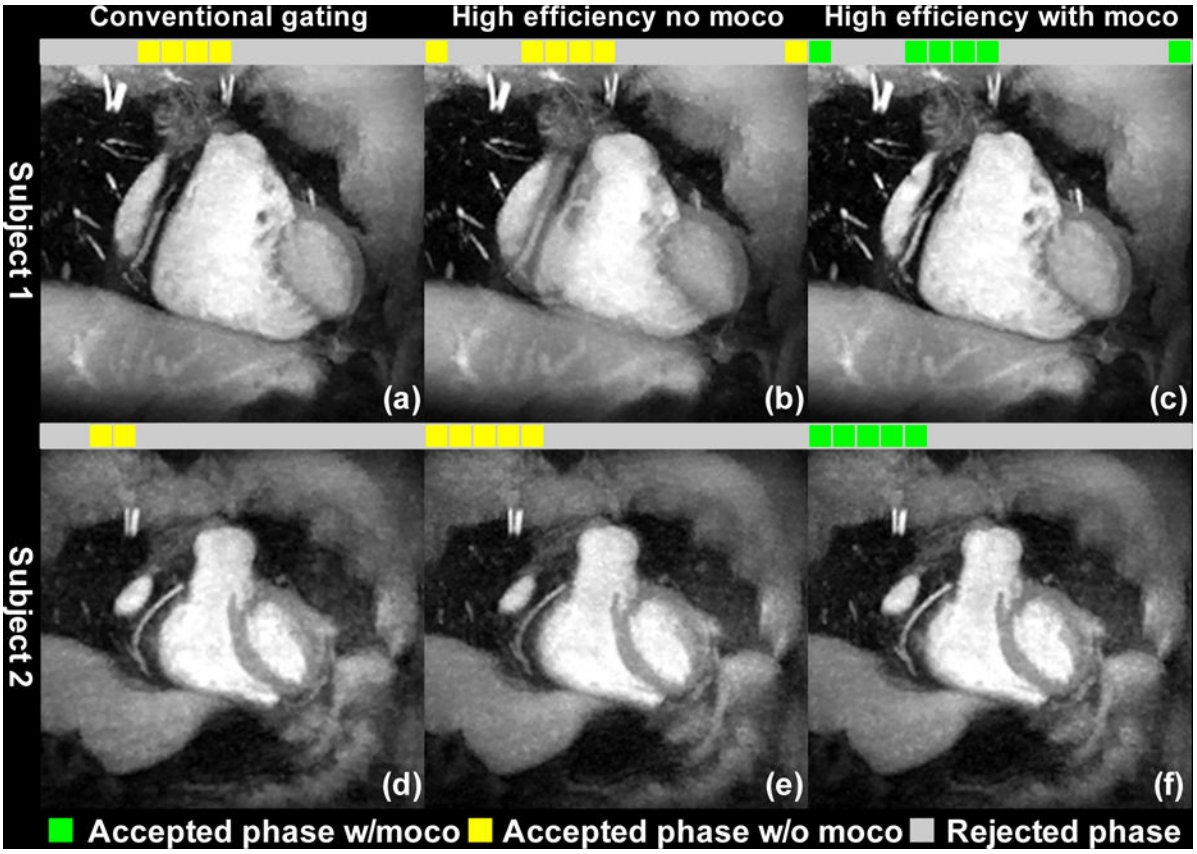

Fig. 4.

Coronal maximum-intensity projection (MIP) images from three reconstructions of two example datasets: (a)(d) conventional gating without motion correction, (b)(e) combining all quiescent phases, without motion correction, and (c)(f) combining all quiescent phases, with motion correction. For subject 1, the accepted phases included ones from both systole and diastole. For subject 2, all phases were from systole, with considerable inter-phase motion within the extended acceptance window. For both subjects, the proposed method improved the image quality over conventional gating by making use of the additional data, while suppressing motion artifacts through effective motion correction.

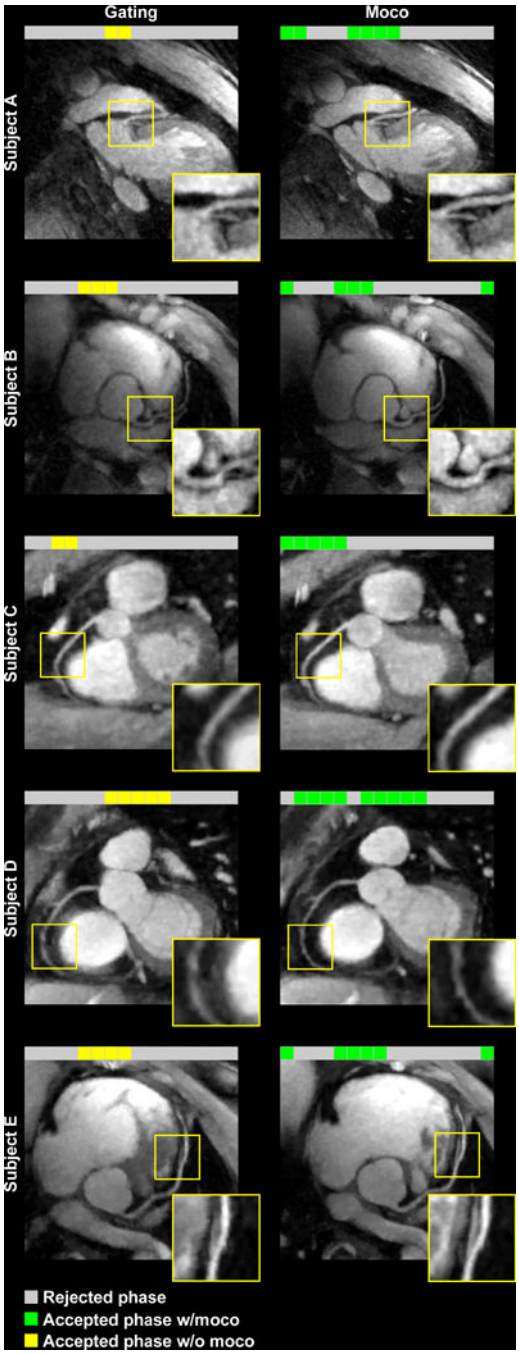

Fig. 5.

Five example subjects comparing conventional cardiac gating (left) with the proposed method (right). The proposed method significantly improved the quality of coronary visualization.

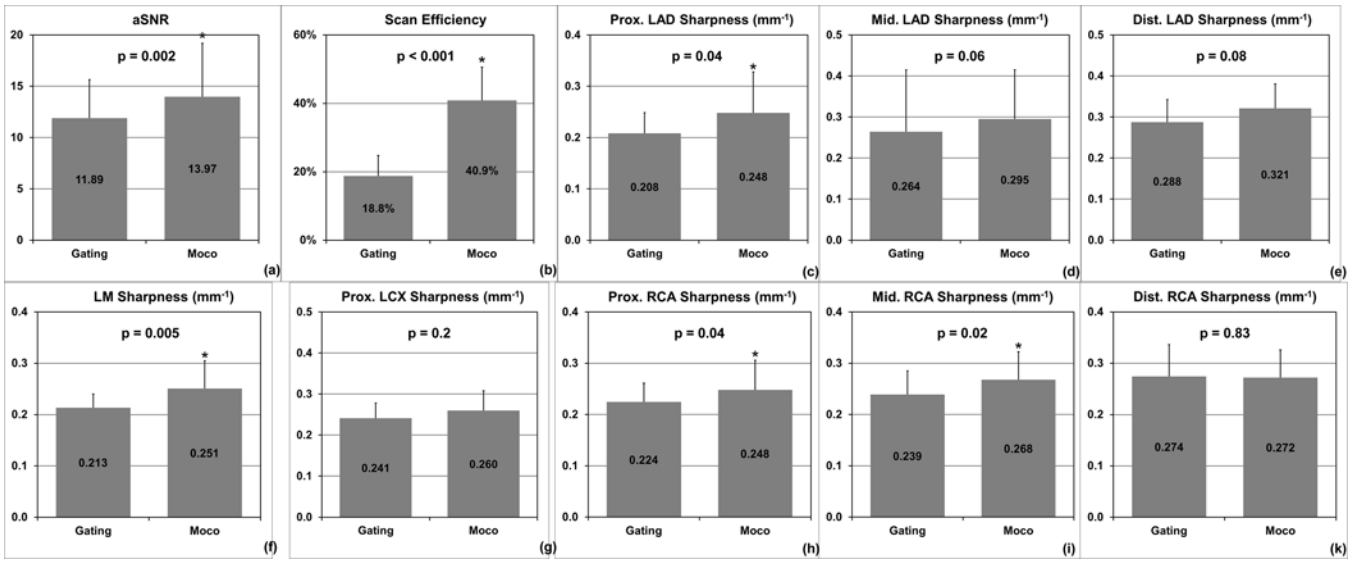

Fig. 6.

Quantitative comparisons of image quality metrics and scan efficiency of the two reconstructions: (a) the proposed reconstruction from the extended acceptance window significantly increased aSNR compared with conventional gating with a smaller window; (b) the extended acceptance window more than doubled the scan efficiency; (c–k) the proposed method significantly improved the sharpness of LM, proximal and middle RCA, and proximal LAD compared with conventional gating.